PLOS ONE

RESEARCH ARTICLE

Genetic diversity and connectivity in the East African giant mud crab *Scylla serrata*: Implications for fisheries management

Cyrus Rumisha[1,2]*, Filip Huyghe[2], Diary Rapanoel[2], Nemo Mascaux[2], Marc Kochzius[2]

1 Sokoine University of Agriculture, Solomon Mahlangu College of Science and Education, Department of Biosciences, Morogoro, Tanzania, **2** Vrije Universiteit Brussel, Department of Biology, Marine Biology, Brussels, Belgium

* cyrus.rumisha@gmail.com, rumisha@suanet.ac.tz

Citation: Rumisha C, Huyghe F, Rapanoel D, Mascaux N, Kochzius M (2017) Genetic diversity and connectivity in the East African giant mud crab *Scylla serrata*: Implications for fisheries management. PLoS ONE 12(10): e0186817. https://doi.org/10.1371/journal.pone.0186817

Editor: Tzen-Yuh Chiang, National Cheng Kung University, TAIWAN

Received: June 8, 2017

Accepted: October 9, 2017

Published: October 24, 2017

Data Availability Statement: All relevant data are within the paper. The COI sequences were submitted to GenBank (https://www.ncbi.nlm.nih.gov/genbank). Accession numbers are included in the manuscript; accession numbers for haplotypes 1–57 = MF496045–MF496101).

Funding: The study was funded by the Vlaamse Interuniversitaire Raad-Universitaire Ontwikkelingssamenwerking (Project Identification Number: ICP PhD 2013-009) through a scholarship given to the first author. The funder

Abstract

The giant mud crab *Scylla serrata* provides an important source of income and food to coastal communities in East Africa. However, increasing demand and exploitation due to the growing coastal population, export trade, and tourism industry are threatening the sustainability of the wild stock of this species. Because effective management requires a clear understanding of the connectivity among populations, this study was conducted to assess the genetic diversity and connectivity in the East African mangrove crab *S. serrata*. A section of 535 base pairs of the cytochrome oxidase subunit I (COI) gene and eight microsatellite loci were analysed from 230 tissue samples of giant mud crabs collected from Kenya, Tanzania, Mozambique, Madagascar, and South Africa. Microsatellite genetic diversity (H_e) ranged between 0.56 and 0.6. The COI sequences showed 57 different haplotypes associated with low nucleotide diversity (current nucleotide diversity = 0.29%). In addition, the current nucleotide diversity was lower than the historical nucleotide diversity, indicating overexploitation or historical bottlenecks in the recent history of the studied population. Considering that the coastal population is growing rapidly, East African countries should promote sustainable fishing practices and sustainable use of mangrove resources to protect mud crabs and other marine fauna from the increasing pressure of exploitation. While microsatellite loci did not show significant genetic differentiation ($p > 0.05$), COI sequences revealed significant genetic divergence between sites on the East coast of Madagascar (ECM) and sites on the West coast of Madagascar, mainland East Africa, as well as the Seychelles. Since East African countries agreed to achieve the Convention on Biological Diversity (CBD) target to protect over 10% of their marine areas by 2020, the observed pattern of connectivity and the measured genetic diversity can serve to provide useful information for designing networks of marine protected areas.

had no role in study design, data collection and analysis, decision to publish, or preparation of the manuscript.

Competing interests: The authors have declared that no competing interests exist.

Introduction

The giant mud crab (*Scylla serrata*) is widely distributed in the Indo-Pacific and it is the only *Scylla* species found at African shores [1]. The crabs provide an important source of income and food to coastal communities in East Africa [2]. Adult and juvenile mud crabs inhabit muddy estuaries and mangrove ecosystems where they can be found buried in mud or taking shelter in burrows at low tide [3,4]. Mated females migrate offshore to spawn because offshore waters provide optimum salinity for larval development and greater chances for dispersal [5]. After hatching, the planktonic larvae undergo a series of up to five moults for a period of two to three weeks [6]. During this period, the larvae are susceptible of being transported by currents and tides to coastal areas where they settle in sheltered areas among mangroves and seagrass. Therefore, currents and tides can influence larval availability. Stock structure and population persistence depends greatly on successful larval settlement and recruitment into the adult population [4]. Knowledge of the patterns of connectivity between sites is crucial for the identification of genetically meaningful management units.

Settlement and recruitment of marine organisms are complex processes, influenced by the interaction of multiple biotic and abiotic factors which operate at different temporal and spatial scales [7]. To identify suitable areas for settlement, larvae of most crustaceans, including *Scylla serrata*, rely on chemical cues produced by adults, predators, and certain macrophytes [8]. However, the ability of olfactory receptors to detect such cues can be seriously affected by the presence of contaminants in the environment [9]. Stock structure can also be affected by overexploitation and habitat alteration. Due to rapid population growth in coastal areas in East Africa, exploitation of mud crabs and other sea food has increased drastically. The rapidly expanding tourism industry and export trade has also led to increased demand and exploitation of mud crabs in the region [10]. As a result, the preferred market size has decreased consistently from more than 1 kg two decades ago to the current size of 0.5 kg [2]. A previous study reported that mud crab catches in the region are dominated by young crabs of 75 mm carapace length, suggesting that few juveniles are able to recruit into the spawning population [11]. The reduction of the spawning population can have serious effects on genetic diversity and sustainability of the mud crab fishery. The collection of juvenile mud crabs for utilisation in aquaculture [12] also puts more pressure on the wild stock and it is likely to exacerbate overexploitation, because this kind of farming is expanding drastically.

The growing coastal population is also threatening the sustainability of mud crab fisheries due to increased incidences of pollution [13,14], and mangrove degradation [15]. In general, 1.25% of the existing African mangrove forest is lost each year [16]. Habitat loss and fragmentation can influence the genetic structure of populations by limiting dispersal capabilities of species [17], which leads to reduced fitness of the population and cases of localised extinction. Although giant mud crabs have very high dispersal capacities [4], they might, over time, suffer these consequences [18]. Such consequences were reported in other mangrove fauna in the region [19,20]. Since genetic diversity is the basis for adaptation, management of genetic diversity is crucial for maintaining the sustainability of marine resources. However, conservation and management of genetic diversity require a clear understanding of the pattern of connectivity among populations.

In 2010, East African countries agreed to implement the UN Convention on Biological Diversity (CBD) strategic plan for biodiversity 2011–2020, which targets to protect over 10% of marine areas by 2020 [21]. Efforts have been taken because up to now, 8.7% of the continental shelf in Kenya, 8.1% in Tanzania, and 4.0% in Mozambique have been designated as marine protected areas (MPAs) [22]. The MPAs provide spatial escape for intensely exploited species, act as buffers against management miscalculations and unforeseen or unusual conditions, and

they are expected to act as centres for dispersion of propagules to surrounding areas [23]. Assessment of the effectiveness of the existing MPAs and establishment of new MPAs require a clear understanding of the patterns of connectivity in the study area. Recent studies did not detected significant genetic differentiation among populations of fiddler crabs *Uca annulipes* [24] and littorinid gastropods (*Littoraria scabra* and *Littoraria glabrata*) [25] along the East African coast. The significant genetic differentiation among the East African *S. serrata* populations documented in a previous study [26] was not confirmed in a more recent study which used a larger number of individuals [27]. Both studies used a fragment (535 base pairs) of the mitochondrial cytochrome oxidase subunit I gene (COI) to analyse genetic variability and connectivity. In order to obtain a better resolution of the genetic population structure of *S. serrata* in the WIO, the present study was conducted using both mitochondrial and microsatellite DNA markers.

Materials and methods

Study area

The study was conducted in East African coastal waters. This coastal zone is characterised by mangrove forests, fringing coral reefs, sand beaches, and rock outcrops [28]. Molluscs, mudskippers, sesarmid crabs, fiddler crabs, and giant mud crabs are commonly found in the mangrove forests [29,30]. The climate of the region has two alternating and distinctive seasons, influenced by the southern and the northern monsoons, which have a marked effect on winds, rainfall, as well as air and water temperature [1]. Ocean currents are driven by trade winds, which are greatly influenced by the movement of the thermal equator (intertropical convergence zone). The currents have a direct influence on nutrient transport and potentially on larval dispersal. The westward South Equatorial Current (SEC) splits at around 17˚S in front of the East coast of Madagascar and flows northward as the Northeast Madagascar Current (NEMC) and southward as the Southeast Madagascar Current (SEMC) [31]. The extension of the SEC northwest of Madagascar reaches the African coast around 11˚S, where it splits into the northward East African Coast Current (EACC) and the southward Mozambique Current (MC) [32]. Flow in the Mozambique channel is dominated by eddies which propagate southward into the Agulhas Current (AC) (Fig 1).

Sampling

Sampling of giant mud crabs (*S. serrata*) was conducted between 2011 and 2015. Tissue samples of 230 individual giant mud crabs were collected from mangrove forests in Kenya, Tanzania, Mozambique, Madagascar, and South Africa (Fig 1 and Table 1). The mud crabs were collected at low tide with the help of local fishermen or bought at landing sites. A section of the pereopod tissue was collected from each animal and preserved in 99.9% ethanol for further analysis.

Ethics statement

Permission to collect samples was provided by the Tanzania Commission for Science and Technology (COSTEC), Tanzania Ministry of Agriculture, Livestock and Fisheries, the University of Tuléar (Madagascar), and the School of Marine and Coastal Sciences, Eduardo Mondlane University.

Laboratory analyses

DNA extraction. Total DNA was extracted from the collected tissues (20–30 mg) by using the E.Z.N.A. Tissue DNA Kit (Omega Bio-Tek Inc., Norcross, USA). Tissue lysis, DNA

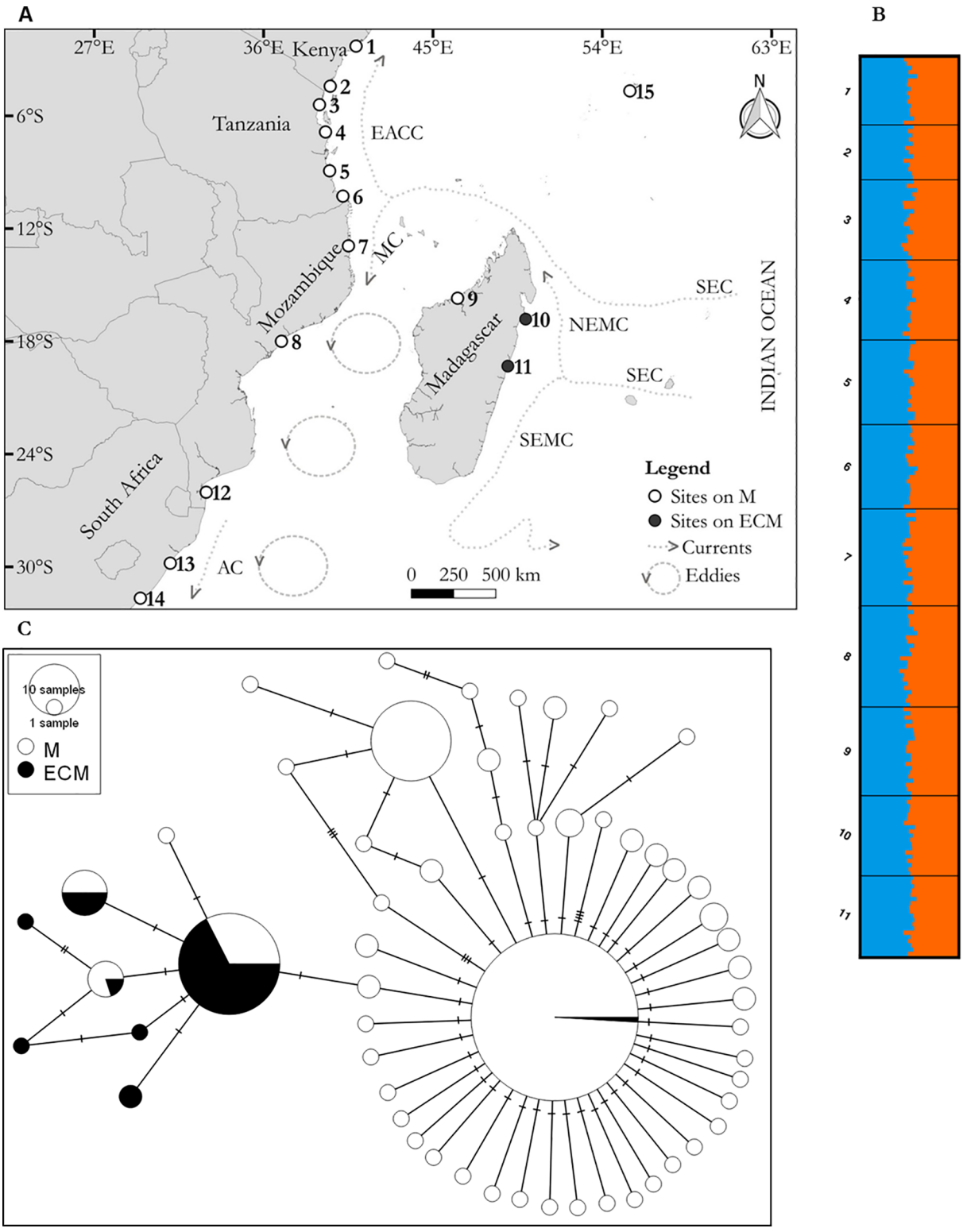

Fig 1. **A**. Map of the East African coast showing sample sites. SEC = South Equatorial Current, EACC = East African Coast Current, MC = Mozambique Current, NEMC = Northeast Madagascar Current, SEMC = Southeast Madagascar Current, AC = Agulhas Current. Main ocean currents were drawn according to [31]. **B**. Bar charts showing the likelihood of individual genotypes of belonging to different groups inferred by STRUCTURE analysis. **C**. Haplotype network of partial cytochrome oxidase subunit I sequences. Each circle represents a haplotype. Size of each circle is proportional to the number of individuals carrying

each haplotype. The central haplotype represents 109 sequences. Hatch marks = mutations. EA = sites on mainland East Africa, West coast of Madagascar, and Seychelles. ECM = East Coast of Madagascar.

https://doi.org/10.1371/journal.pone.0186817.g001

extraction, and purification were performed according to the manufacturer's protocol. Agarose gel electrophoresis was performed to check the quality of the DNA extracts. Agarose gel electrophoresis was performed using the procedures outlined in a previous study [20].

Polymerase chain reactions. Polymerase chain reactions (PCR) were performed using an MJ research PTC 200 Peltier thermocycler. Multiplex PCR was performed to assess microsatellite polymorphism. Two multiplex systems containing eight microsatellite markers were developed using previously published markers (Table 2)[34–36]. The software Multiplex Manager ver. 1.2 [37] was used to organise the primers into two multiplex sets. Multiplex PCR reactions were performed using the Type-it Microsatellite PCR Kit (QIAGEN Inc., Valencia, CA, USA). Optimisation and thermocycling profiles were conducted according to the manufacturer's protocol. Agarose gel electrophoresis was performed to assess yield and quality of the PCR products. Fragment analysis was performed by using an Applied Biosystems 3730 capillary sequencer. GeneScan 500 LIZ was used as a size standard. The obtained microsatellite fragments were genotyped with the software GeneMarker ver. 2.2.0 (SoftGenetics LLC, Oakwood, USA). The program CONVERT ver. 1.3.1 [38] was used to reformat the obtained genotypic data in order to generate input files for population genetic software packages used in subsequent analyses. PCR and fragment analysis were repeated for samples that produced unclear genotypes.

A fragment (557 bp) of the COI gene was also amplified using the primers mtd10 5´ TTGATTTTTTGGTCATCCAGAAGT 3´ [39] and C/N 2769 5´ TTAAGTCCTAGAAATGTTRGGGA 3´ [33]. The PCR were done in a total volume of 25 μL containing 10 ng of the DNA template, 0.25 U of the *Thermus aquaticus* DNA polymerase, 0.2 μM of each primer, 0.2 mM DNTP,

Table 1. Number of giant mud crabs (*Scylla serrata*) collected from mangrove forests at the Western Indian Ocean. COI = Cytochrome oxidase subunit I sequences analysed, COI previous study = COI sequences taken from previous studies [27,33].

Site	Site name	Coordinates		Samples		
		Longitudes (˚ E)	Latitudes (˚ S)	Microsatellite Samples	COI this study	COI previous studies
1	Lamu, Kenya	40.91	2.29	16	14	30
2	Gazi, Kenya	39.54	4.42	13	14	30
3	Pangani, Tanzania	38.97	5.41	32	31	-
4	Dar es Salaam, Tanzania	39.29	6.86	20	20	-
5	Kilwa, Tanzania	39.51	8.93	20	20	-
6	Mtwara, Tanzania	40.21	10.27	20	20	-
7	Pemba, Mozambique	40.51	12.92	23	22	-
8	Quelimane, Mozambique	36.95	18.00	24	25	-
9	Mahajanga, Madagascar	46.31	15.70	21	21	-
10	St Marie, Madagascar	49.93	16.82	19	18	-
11	Vatomandry, Madagascar	48.98	19.32	19	20	-
12	Inhaca, Mozambique	32.95	26.03	-	-	28
13	Durban, South Africa	31.04	29.81	-	-	11
14	Kwa Zulu Natal, South Africa	29.45	31.67	-	5	
15	Mahe island, Seychelles	55.47	4.67	-	-	26
	Total			**227**	**230**	**125**

https://doi.org/10.1371/journal.pone.0186817.t001

Table 2. Primers used to amplify microsatellite loci in the giant mud crab *Scylla serrata* from the Western Indian Ocean. Cy3 = Cyanine3. Dye = fluorescent dye, Na = number of alleles, Ta = annealing temperature.

	Locus	Repeat motif	Primer sequence (5'-3')	Size (bp)	Na	Dye
Multiplex 1 (Ta = 50˚C)	Scpa-INI-SSR	$(AG)_{31}$	F: CTGTCTGTCCCTCGCGTCC	167–215	22	HEX
			R: TTCTCTCCCTTTTGAGCGAATAAG			
	Scse53-1	$(CA)_{32}$	F: CCGTCACTTCACAGTATA	236–240	2	Cy3
			R: GTTTTCATTTGAGTTTCC			
	Scse43-1	$(TG)_{15}$	F: GAAATCTGAGCTGCCAATC	222–240	10	ROX
			R: CACCCATCCAAGTACCAA			
Multiplex 2 (Ta = 54.2˚C)	Scse96-1	$(GAAGG)_{10}$	F: CTTCCTCACCGTCCCTAT	270–285	4	6FAM
			R: CTCTGTTGCCTAATTCCTC			
	Scpa-CB-SSR	$(TG)_{17}$	F: CAGTGCAAGGCAAGTCAGGATAC	264–296	15	ROX
			R: AGTTCTGGAAGCATGCAATACTGAC			
	SCY38	(CA)14	F: CAGACACTCAAGTCTCACCTGC	233–245	7	HEX
			R: CAGAATGGTTAATGGGGGG			
	SCY12	(CA)16	F: AGACCTCTCTCCCTTCCTGC	201–211	6	Cy3
			R: GGTGAACCTGCTTGGCAC			
	SCY23	(CA)11	F: TGACAGTTGGTAGAGGCGC	113–117	3	Cy3
			F: GTCTAGCTGAGAGGGCGATG			

https://doi.org/10.1371/journal.pone.0186817.t002

3 mM $MgCl_2$, 1x Taq buffer, and 0.4 mg bovine serum albumin. The PCR profiles included an initial denaturation step of 5 min at 95˚C, followed by 35 cycles of 30 s at 95˚C, 30 s at 50˚C, and 1 min at 72˚C. A final extension step of 10 min at 72˚C was added to ensure complete amplification. Agarose gel electrophoresis was performed to assess the quality of the PCR products. Sequencing of both strands of the fragment of COI gene was done with an ABI 3700 XL sequencer. For each sample, the obtained forward and reverse sequences were edited and aligned using the ClustalW algorithm as implemented in MEGA ver. 6.0 [40] to generate consensus sequences (557 base pairs). The same software was used to translate the nucleotide sequences into amino acid sequences using the invertebrate mitochondrial genetic code. This was done in order to ensure that functional mitochondrial DNA was obtained and not a nuclear pseudogene [41].

Data analyses

Analysis of genetic diversity. Microsatellite based estimates of the observed and expected heterozygosity were determined with the software GenAlEx ver. 6.5 [42]. The same software was used to test for departure from the Hardy-Weinberg equilibrium (HWE). Allelic richness was estimated with the program FSTAT ver. 2.9.3 [43]. The same program was used to estimate F_{IS} (within sub-population inbreeding coefficient) and to test whether it is significantly different from zero. Prior to these analyses, samples with missing data at three or more loci were removed from the data set. The data set was also checked for null alleles, large allele drop out, and scoring errors due stuttering using the software Micro-Checker ver. 2.2 [44].

A total of 230 COI sequences were obtained from the analysed tissues. Alignment of the edited sequences was performed with MEGA ver. 6.1 [40] to generate a multiple alignment with 535 base pairs. Estimates of genetic diversity, such as the number of haplotypes, haplotype diversity, current nucleotide diversity (θ_π, based on pairwise differences), and historical nucleotide diversity (θ_w, based on number of segregating sites) were calculated with the program DnaSP ver. 5.10 [45].

Population structure and demographic history. The analysis of molecular variance (AMOVA) of the microsatellite data was performed with the software Arlequin ver. 3.5.1.2 [46], in order to determine the pattern of differentiation between sample sites. Since the markers displayed multiple alleles, correlation analysis between the single locus G_{ST} values and the within subpopulation genetic diversity (Hs) was performed using the computer program CoDiDi (Correlation between Diversity and Differentiation) ver. 1.0 [47]. This was done in order to determine if G_{ST} is an appropriate measure of genetic differentiation for the sampled populations. Generally, G_{ST} gives correct estimates of genetic differentiation if the effect of mutation is lower than other demographic forces. Mutation effects are lower than other demographic factors when the correlation between G_{ST} and Hs (within subpopulation expected heterozygosity) is not significant [47]. Pairwise comparison of G_{ST} was performed with GenAlEx ver. 6.5 [42], in order to determine the pattern of genetic differentiation between populations. The significance of G_{ST} values was determined according to the Holm-Bonferroni sequential procedure [48]. To test whether individuals clustered according to geographical origin, a Bayesian analysis implemented in the software STRUCTURE ver. 2.3.4 [49] was performed, testing for different numbers of clusters (k) in the dataset and giving the corresponding probabilities. STRUCTURE HARVESTER ver. 0.6.94 was used to infer the optimal k through the Δk statistic, which is based on the rate of change of log probability of the data between successive k–values [50].

The 230 analysed COI sequences were combined with 125 previously published sequences [27,33], to form a combined data set with 355 sequences (Table 1). The software MEGA ver. 6.0 [40] was used to align the sequences. The program FaBox DNA collapser ver. 1.41 [51] was used to collapse the aligned sequences into haplotypes and to create input files for subsequent analyses. Analysis of Molecular Variance (AMOVA) of the sequences was performed in order to analyse the partitioning of the total genetic variation and to estimate the fixation index. This was done by using the software Arlequin ver. 3.5.1.2 [46]. The same software was used to compare populations by computing pairwise F_{ST} values, which were calculated from haplotype frequencies. The significance of pairwise F_{ST} values was calculated by 10,000 random permutations of haplotypes between populations. The F_{ST} p-values were adjusted using the Holm-Bonferroni sequential procedure [48]. Hierarchical AMOVA was performed to determine if there is a significant genetic break between groups of populations. The significance of the population fixation indices (F_{ST} and Φ_{ST}) was determined with 10,000 permutations. A minimum spanning haplotype network was constructed with the software PopART ver. 1.7 [52] to examine the relationship between haplotypes. The mutation-scaled effective population size Θ ($2Ne\mu$) and the mutation-scaled migration rates ($M = m/\mu$) (where Ne = effective population size, m = immigration rate per generation, μ = mutation rate per generation) were estimated using the program MIGRATE-N ver. 3.6.11 [53]. The program was run based on a full migration matrix model and Bayesian inference. The parameters Θ and M were estimated based on an exponential posterior distribution and a single long chain run consisting of 50 000 recorded steps, burn-in of 100 000, and four heated chains (static heating scheme) with temperatures 1.00, 1.50, 3.00 and 1 000 000. Prior to this, three replicate runs (without heating) were performed to estimate the boundaries of Θ and M. The number of immigrants per generation ($2Nem$) was obtained by multiplying Θ and M [53].

Fu's Fs [54] and Tajima's D [55] tests of neutrality were performed to evaluate the demographic history of the studied populations. Mismatch distribution analysis was performed to estimate the parameters of the sudden expansion model such as the sum of the squared deviation, the Harpending's Raggedness index, and the time since expansion [56].

Results

Genetic diversity

The eight analysed microsatellite loci did not show significant evidence of large allele drop out or scoring errors due to stuttering. In addition, the analysed loci did not show significant evidence of null alleles in all sampled populations, except locus Scse43-1 at site 4. The loci Ssse96-1 and Scpa-INI-SSR showed significant deviation from the HWE at site 3. The locus Scse43-1 showed significant departure from the HWE at sites 4 and 7. Significant departure from the HWE was also shown by the loci SCY38 and SCY12 at sites 6 and 10, respectively. The locus Scse53-1 was monomorphic at all sites, except site 1 (Table 2). The total number of alleles ranged between 2 and 22. Expected heterozygosity ranged between 0.561 and 0.601 (Table 3). The within sub-population inbreeding coefficients (F_{IS}) were not significantly different from zero ($p > 0.00057$ (adjusted nominal level)).

A total of 230 COI sequences each with 535 base pairs were obtained. Diversity indices were calculated only for sites with at least 14 sequences. The analysed sequences showed 40 haplotypes. The highest haplotype diversity was observed at sites 2 and 8 (Table 4). The lowest haplotype diversity was measured in samples from site 11. The current nucleotide diversity was generally low as it ranged between 0.07% (site 11) and 0.32% (site 8). In addition, the current nucleotide diversity was generally low than the historical nucleotide diversity ($\theta_\pi < \theta_w$).

Demographic history

A multiple alignment of the 230 sequences obtained during this study and the 125 previously published COI sequences was performed. The sequences were collapsed with the program FaBox DNA collapser ver. 1.41 [51] to generate 57 haplotypes (Table 5). The haplotype sequences were submitted to GenBank (accession numbers for haplotypes 1–57 = MF496045—MF496101). Fu's Fs and Tajima's D test of the pooled samples showed significant deviation from the neutral evolution hypothesis (Tajima's D = -2.36, $p < 0.001$: Fu's Fs = -27.48, $p < 0.001$). Mismatch distribution of the pooled samples produced a unimodal distribution, supporting the null hypothesis of population expansion (Fig 2). The raggedness index and sum of squared deviations (SSD) showed that the null hypothesis of population expansion cannot be rejected (raggedness index = 0.025, $p > 0.05$: SSD = 0.00087; $p > 0.05$). Fu's Fs and Tajima's D test were also performed for each population and they indicated significant deviation from

Table 3. Indices of microsatellite genetic diversity in the East African giant mud crab *Scylla serrata*. N = sample size, Ar = allelic richness, H_o = observed heterozygosity, H_e = expected heterozygosity, F_{IS} = within sub population inbreeding coefficient. Cy3 = Cyanine3. For sites see Table 1 and Fig 1.

Site	N	Ar	H_o	H_e	F_{IS}
1	16	4.5	0.57	0.591	0.04
2	13	4.5	0.61	0.587	-0.04
3	32	4.9	0.57	0.596	0.04
4	20	4.5	0.61	0.597	-0.02
5	20	4.2	0.64	0.561	-0.14
6	20	4.5	0.53	0.583	0.10
7	22	4.8	0.59	0.593	0.00
8	24	4.9	0.59	0.601	0.01
9	19	4.3	0.58	0.583	0.00
10	18	3.9	0.54	0.576	0.07
11	21	3.7	0.58	0.567	-0.01

https://doi.org/10.1371/journal.pone.0186817.t003

Table 4. Indices of molecular diversity in the East African giant mud crab *Scylla serrata* based on mitochondrial cytochrome oxidase subunit I sequences. N = sample size, n_h = number of haplotypes, h = haplotype diversity, θ_π = current nucleotide diversity, θ_w = historical nucleotide diversity. For sample sites, see Fig 1 and Table 1.

Sites	1	2	3	4	5	6	7	8	9	10	11	Total
N	14	14	31	20	20	20	22	25	21	18	20	**225**
n_h	5	7	10	4	8	5	5	11	9	8	3	**40**
h	0.59	0.85	0.66	0.28	0.59	0.66	0.62	0.85	0.65	0.64	0.35	**0.75**
θ_π (%)	0.26	0.29	0.22	0.13	0.18	0.24	0.18	0.32	0.19	0.22	0.07	**0.29**
θ_w (%)	0.41	0.29	0.52	0.32	0.42	0.37	0.31	0.50	0.53	0.44	0.11	**1.15**

https://doi.org/10.1371/journal.pone.0186817.t004

the hypothesis of neutral evolution for all sampled populations, except populations at sites 6, 7, 11, 13, 14, and 15 (Table 6). The raggedness index for each population was not significant except for the population at site 8.

Table 5. Distribution of the cytochrome oxidase subunit I haplotypes in the East African giant mud crab *Scylla serrata*. The number below each haplotype is proportional to the number of individuals carrying each haplotype, n_h = number of haplotypes (GenBank accession numbers for haplotypes 1–-57 = MF496045—MF496101).

Site	n_h	Distribution of haplotypes																
1	12	h1	h10	h11	h12	h13	h16	h17	h18	h19	h26	h27	h28					
		30	4	1	1	1	1	1	1	1	1	1	1					
2	17	h1	h2	h3	h4	h5	h6	h7	h8	h9	h10	h14	h15	h27	h29	h30	h31	h32
		20	1	1	1	1	1	1	1	2	5	1	2	3	1	1	1	1
3	9	h1	h5	h10	h33	h34	h35	h36	h41	h43								
		18	1	4	1	1	1	1	2	1								
4	4	h1	h36	h37	h38													
		17	1	1	1													
5	8	h1	h10	h30	34	h39	h40	h41	h42									
		13	1	1	1	1	1	1	1									
6	5	h1	h10	h13	h19	h27												
		11	3	1	1	4												
7	5	h1	h11	h15	h37	h44												
		12	1	1	7	1												
8	11	h1	h15	h27	h30	h31	h40	h45	h46	h47	h48	h49						
		4	1	9	2	1	1	1	2	1	1	2						
9	9	h1	h15	h27	h33	h45	h54	h55	h56	h57								
		13	1	1	1	1	1	1	1	1								
10	8	h1	h10	h15	h30	h50	h51	h52	h53									
		1	11	1	1	1	1	1	1									
11	3	h10	h15	h52														
		16	3	1														
12	8	h1	h10	h15	h19	h20	h21	h22	h23									
		18	3	1	1	1	1	2	1									
13	1	h1																
		11																
14	2	h1	h5															
		4	1															
15	5	h1	h7	h10	h24	h25												
		18	1	5	1	1												

https://doi.org/10.1371/journal.pone.0186817.t005

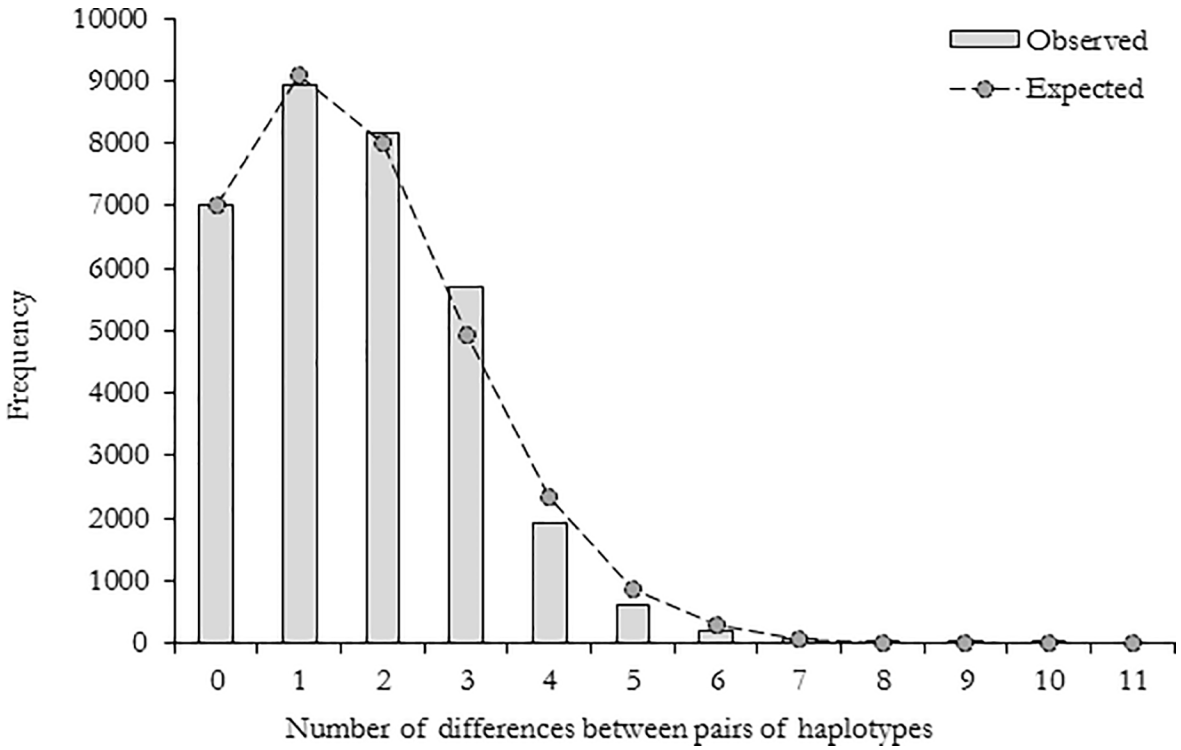

Fig 2. Pairwise mismatch distribution showing a unimodal distribution of the cytochrome oxidase subunit I haplotypes in the East African giant mud crab *Scylla serrata*.

https://doi.org/10.1371/journal.pone.0186817.g002

Connectivity among populations

Correlation analysis showed that the association between the microsatellite based genetic differentiation (G_{ST}) and the within subpopulation expected heterozygosity (Hs) is not significant (G_{ST} = 0.0093Hs—0.0023: r = 0.327, $p > 0.05$). The analysis of molecular variance of the microsatellite data showed that the variation among sites was not significant (F_{ST} = 0.00424, $p > 0.05$, 100172 permutations). STRUCTURE analysis did not detect meaningful genetic clusters (Fig 1). Apart from that, the analysis of molecular variance (AMOVA) of the COI sequences revealed significant genetic differentiation among sites (F_{ST} = 0.158, $p < 0.001$; Φ_{ST} = 0.238, $p < 0.001$). Pairwise comparison of F_{ST}-values showed variable connectivity

Table 6. Parameters estimated under the selective neutrality tests and the sudden expansion model for the East African giant mud crab (*Scylla serrata*) based on cytochrome oxidase subunit I sequences. D = Tajima's D, FS = Fu's FS, HRI = Harpending's raggedness index, SSD = sum of squared deviations, p = p-values. For sample sites, see Table 1 and Fig 1.

Sites	1	2	3	4	5	6	7	8	9	10	11	12	13	14	15
D	**-2.4**	**-1.9**	**-1.8**	**-1.9**	**-1.9**	-1.2	-1.3	-1.1	**-2.3**	**-1.7**	-0.8	**-1.7**	0.0	-0.8	-0.9
D p	0.00	0.01	0.01	0.01	0.01	0.12	0.08	0.13	0.00	0.02	0.25	0.02	1.00	0.29	0.20
FS	**-7.2**	**-13.7**	**-5.7**	-0.8	**-5.1**	-0.5	-1.2	**-5.8**	**-6.8**	**-4.6**	-0.8	**-3.8**	0.0	0.1	-1.1
FS p	0.00	0.00	0.00	0.24	0.00	0.33	0.14	0.00	0.00	0.00	0.20	0.00	N.A.	0.30	0.15
SSD	**0.39**	0.00	0.00	0.01	0.00	0.01	0.01	0.03	0.01	0.01	0.00	0.00	0.00	0.01	**0.36**
SSD p	0.00	0.60	0.85	0.36	0.80	0.57	0.21	0.07	0.32	0.58	0.47	0.86	0.00	0.79	0.00
HRI	0.2	0.0	0.0	0.3	0.1	0.1	0.1	**0.2**	0.1	0.0	0.2	0.0	0.0	0.2	0.2
HRI p	0.98	0.63	0.96	0.56	0.86	0.82	0.26	0.02	0.35	0.99	0.40	0.90	0.00	0.94	1.00

https://doi.org/10.1371/journal.pone.0186817.t006

Table 7. Pairwise F_{ST}-values derived from pairwise comparison of cytochrome oxidase subunit I sequences of giant mud crabs (*Scylla serrata*) in the Western Indian Ocean. Bold values are significant after Holm-Bonferroni sequential correction. For sample sites, see Table 1 and Fig 1.

Sites	1	2	3	4	5	6	7	8	9	10	11	12	13	14
2	0.03													
3	0	0												
4	0.02	0.10	0.06											
5	-0.02	0.01	-0.02	0.02										
6	0.01	-0.01	0.00	0.11	0.01									
7	0.07	0.03	0.06	0.15	0.06	-0.01								
8	**0.23**	0.09	**0.17**	**0.33**	**0.19**	0.10	0.07							
9	-0.01	0.01	-0.01	0.04	-0.02	0.01	0.03	**0.16**						
10	**0.36**	**0.20**	**0.27**	**0.52**	**0.34**	**0.26**	**0.35**	**0.24**	**0.34**					
11	**0.50**	**0.34**	**0.42**	**0.68**	**0.51**	**0.42**	**0.50**	**0.38**	**0.50**	0.01				
12	-0.01	0.01	-0.01	0.04	-0.02	0.01	0.07	**0.20**	-0.01	**0.32**	**0.47**			
13	0.07	0.17	0.13	0.01	0.10	0.19	0.23	**0.40**	0.11	**0.60**	**0.78**	0.10		
14	-0.05	0.01	-0.03	-0.04	-0.06	0.01	0.05	0.21	-0.05	0.41	**0.63**	-0.04	0.17	
15	-0.01	0.03	-0.01	0.04	-0.01	0.02	0.10	**0.24**	0.02	**0.33**	**0.49**	-0.01	0.11	-0.02

https://doi.org/10.1371/journal.pone.0186817.t007

among the sample sites. With the exception of site 8, populations from Seychelles, Kenya, Tanzania, Mozambique, South Africa, and the West Coast of Madagascar did not show significant genetic differentiation (Table 7). Apart from that, a significant genetic break was observed for populations on the East coast of Madagascar (ECM) (sites 10 and 11), which were significantly differentiated from the other sample sites. This was confirmed by hierarchical AMOVA, which showed significant genetic differentiation between populations on the ECM and other sampled populations ($F_{CT} = 0.361$, $p < 0.01$: $\Phi_{CT} = 0.564$, $p < 0.01$). The observed pattern of genetic differentiation was also revealed in the haplotype network (Fig 1). The network showed a star-like shape, with two main clusters of haplotypes joined to the main haplotype by few mutations. Haplotypes of populations on the ECM formed a separate cluster, which contained very few shared haplotypes (4 shared haplotypes and 4 private haplotypes). Sites from Kenya, Tanzania, and the Mozambique Channel showed high effective population size compared to other sites (Table 8). Estimates of the immigration rate showed high rate of immigration to Kenyan and Tanzanian mangroves and the lowest immigration rate to mangroves at the ECM.

Discussion

Genetic diversity

The East African *S. serrata* populations showed high mitochondrial DNA haplotype diversity and low nucleotide diversity (Table 4). This is due to the fact that most haplotypes differed from each other by very few mutations (one to five mutations, S1 Table). Similar observations were previously reported in *S. serrata* in the WIO [26,27] and the Western Pacific [33]. Similar findings were also reported in other mangrove fauna in the WIO [19,24]. The high haplotype diversity and low nucleotide diversity might indicate genetic bottleneck events, where most haplotypes became extinct, followed by population expansion [57]. The measured haplotype diversity ($h = 0.75$) and nucleotide diversity ($\theta_\pi = 0.29\%$) are low compared to the reported levels of genetic diversity in the mangrove crabs *Uca hesperiae* ($h = 0.80 \pm 0.02$, $\theta_\pi = 0.25 \pm 0.16\%$), *Perisesarma guttatum* ($h = 0.85 \pm 0.02$, $\theta_\pi = 0.42 \pm 0.25\%$), and *Neosarmatium africanum* ($h = 0.82 \pm 0.02$, $\theta_\pi = 0.46 \pm 0.26\%$) [58] from the WIO. Nevertheless, the measured indices of genetic diversity are higher than the reported levels of genetic diversity in the mangrove crab *Uca occidentalis* ($h = 0–0.679$, $\theta_\pi = 0–0.13\%$ [24]: $h = 0.19 \pm 0.03$, $\theta_\pi = 0.03 \pm 0.04\%$ [58])

Table 8. Mutation-scaled effective population size (Θ) and the mutation-scaled immigration rates (M = m/μ) in the giant mud crabs *(Scylla serrata)* from the Western Indian Ocean. Migrants = number of immigrants (Θ times M). Group A = sites in Kenya and Tanzania, B = sites in the Mozambique channel, C = sites on the ECM, D = site 12–14, E = Seychelles.

Groups	Θ	Direction	M	Migrants	Total immigrants	Total emigrants
A	0.0445	B → A	300.5	4	7	10
B	0.0125	C → A	156.7	0	4	6
C	0.0028	D → A	432.4	3	3	2
D	0.0058	E → A	384.8	1	4	4
E	0.0017	A → B	66.1	3	4	1
		C → B	109.9	0		
		D → B	144.9	1		
		E → B	129.7	0		
		A → C	52	2		
		B → C	42.7	1		
		D → C	61.6	0		
		E → C	68.9	0		
		A → D	63.5	3		
		B → D	54.2	1		
		C → D	198.2	1		
		E → D	151.6	0		
		A → E	53.8	2		
		B → E	60.1	1		
		C → E	119.2	0		
		D → E	70.4	0		

https://doi.org/10.1371/journal.pone.0186817.t008

from the WIO, but comparable to the reported levels of genetic diversity in *S. serrata* in the WIO [26,27,33,58]. The measured indices of microsatellite diversity are also comparable to reported levels of microsatellite diversity in *Scylla paramamosain* from the East China Sea [36]. Since genetic diversity is the raw material for evolution [59], these findings suggest that the studied population is genetically robust. However, the fact that current genetic diversity was low compared to historical genetic diversity indicates that the studied population experienced periods of overexploitation or historical bottlenecks.

Demographic history

The Fu's Fs and Tajima's D test of the pooled sample showed significant deviation from the neutral evolution hypothesis (Tajima's D = -2.36, $p < 0.001$: Fu's Fs = -27.48, $p < 0.001$). When the hypothesis of neutral evolution was tested for each population, significant departure from the hypothesis were observed at all sampled populations, except the populations at sites 6, 7, 11, 13, 14, and 15 (Table 7). This indicates selection or demographic expansion of the *S. serrata* populations in the study area. Mismatch distribution of the pooled sample produced a unimodal distribution, supporting the null hypothesis of population expansion (Fig 2). The raggedness index and sum of squared deviations (SSD) showed that the null hypothesis of population expansion cannot be rejected (raggedness index = 0.025, $p > 0.05$: SSD = 0.00087; $p > 0.05$). The constructed haplotype network also support the null hypothesis of recent population expansion. The network produced a star like structure, with the central haplotypes surrounded by several haplotypes that show little base pair differences (Fig 1). This suggests that most haplotypes originated recently and it is indicative of recent population expansion from a small number of founders [60]. The time of expansion was estimated from the expansion

parameter tau (τ), using the equation t = τ/2 μ, where μ is the rate of mutation. Using the estimated τ of 1.10625 and the COI mutation rate of 1.15% per million years [33], the time at which population expansion began was estimated to be about 90 thousand years ago. This time corresponds with the last glacial period which spanned from 125 to 14.5 thousands of years ago. The observed population expansion was probably due to sea level oscillations during this time [61].

Connectivity among populations

The correlation between microsatellite genetic differentiation (G_{ST}) and the within subpopulation heterozygosity was not significant ($p > 0.05$). This shows that single loci G_{ST}-values are marker independent and that G_{ST} is the best estimate of genetic differentiation in the study area [47]. Apart from that, AMOVA of the microsatellite data did not detect significant genetic differentiation among sites ($F_{ST} = 0.00424$, $p > 0.05$, 100172 permutations). In contrast, COI showed significant genetic differentiation among sites ($F_{ST} = 0.158$, $p < 0.05$; $\Phi_{ST} = 0.238$, $p < 0.05$). The contrasting patterns of genetic differentiation between nuclear and mitochondrial DNA are reported in several other species [62,63] and they can be due to a complex array of conditions that include selection, fluctuations in populations size, variations in sex ratio, and introgressive hybridisation [62,64]. Introgressive hybridisation from related species, does not account for the observed patterns, since *S. serrata* is the only *Scylla* species occurring in the study area [1]. In addition, the observed discrepancy might not be due to selection, because the neutrality tests showed no evidence of selection in the mtDNA (Table 7). While nuclear DNA is less likely to be affected by bottlenecks and rapid population expansions, mtDNA is more susceptible to these evolutionary forces due to its smaller effective population size [65,66]. Evidence of sudden expansion of the East African *S. serrata* populations was revealed by the mismatch analysis (Fig 2). This suggests that the observed discordance might be due to the varying effects of genetic drift on mitochondria and nuclear DNA. In addition, if there is no variations in sex ratio, the index of genetic differentiation is expected to be four times higher in mtDNA than nuclear DNA [67]. The ratio of mtDNA to nuclear DNA differentiation in the present study was 37 (0.157/0.00424). This suggests that the observed discrepancy in population differentiation between mitochondrial and microsatellite DNA is probably due to variation in sex ratio. Generally, in areas without sex-biased fishery, males giant mud crabs can outnumber females by three folds [68]. This is in line with what was observed during fieldwork, since males showed high abundance. High abundance of male *S. serrata* in East African mangroves was also reported in a previous study [11]. Therefore, the observed discordance is probably due to variation in sex ratio.

The analysis of molecular variance did not detect significant genetic differentiation among sites in the Seychelles, Kenya, Tanzania, Mozambique, and South Africa. The observed lack of genetic differentiation between these sites is in line with the findings of previous studies [27,58]. A similar pattern of genetic differentiation in this region was also reported in other mangrove fauna [24,25,58]. In contrast to these studies, this study detected significant genetic differentiation between sites at the East coast of Madagascar (ECM) and sites in mainland East Africa and the Seychelles ($F_{CT} = 0.361$, $p < 0.05$: $\Phi_{CT} = 0.564$, $p < 0.05$). The fact that previous studies did not include samples from the ECM [24,25,58] can explain why no genetic differentiation was detected in previous studies. The fact that significant genetic differentiation between Mauritius Island and mainland East Africa was not detected in two previous studies [27,33] can be attributed to consequences of low sample size. The studies used only five sequences, representing only one haplotype from Mauritius. The observed genetic break between populations on the ECM and other sample sites is probably due to the influence of

ocean circulation on larval transport and dispersal. Oceanic circulations in the region are influenced by trade and monsoon winds [1]. Because *S. serrata* has a planktonic larval stage, the SEC is expected to transport and disperse larvae from the ECM to East Africa through the EACC, MC and AC. The observed genetic differentiation indicate that there is limited larval exchange between sites in the ECM and sites in mainland East African and the Seychelles. This is supported by the measured mutation scaled immigration rate, which showed lowest rate of immigration to mangroves at the ECM (Table 8). The observed pattern in genetic differentiation is also supported by the haplotype network, which showed haplotypes from the ECM in a separate cluster, containing very few shared haplotypes (Fig 1). The patterns of currents can also account for the lack of genetic differentiation among sites on the coastline of East Africa. Circulation in East African coastal waters are influenced by the northward EACC, as well as the MC and eddies in the Mozambique channel, which propagate southward into the south-bound AC [31]. These currents are probably responsible for the dispersal of larvae among adjacent populations and thus accounting for the observed connectivity. This argument is supported the haplotype network, which showed that mangrove forests in the Mozambique channel, Kenya, Tanzania, South Africa and the Seychelles share the most common haplotypes (Fig 1).

Implications for fisheries management

The study showed that the current genetic diversity is low compared to historical genetic diversity ($\theta_\pi < \theta_w$). This shows that the studied population experienced bottlenecks in its recent history. Considering that indications of mud crab overexploitation and mangrove degradation are reported in the study area [2,11], measures aimed at enhancing sustainable use of resources should be strengthened. The observed limited gene flow between ECM and other sites indicate that protected mangroves and MPAs in the west coast of Madagascar and mainland East Africa cannot help to protect the biodiversity of mangroves in the ECM. Since Madagascar is planning to triple the extent of its MPAs by 2020, the observed patterns provide useful information for establishment of MPA networks around the island. Since giant mud crabs in the WIO are heavily exploited for food and trade, the observed low population size in the ECM and the Seychelles suggest that these areas require immediate attention. The mangroves in Kenya and Tanzania showed a high effective population size, which is maintained by a high rate of immigration from other mangroves in mainland East Africa. Estimates of migration rate showed highest number of immigrants to mangroves in this region (Table 8), indicating that overexploitation and degradation of some ecosystems is likely to affect recruitment and stock structure of adjacent ecosystems. Therefore, management efforts should strive to maintain connectivity among mangroves in this region. Since female giant mud crabs migrate offshore to spawn, management efforts should focus on both intertidal and offshore ecosystems.

Conclusion

East African countries agreed to implement the UN Convention on Biological Diversity (CBD) strategic plan for biodiversity 2011–2020, which is targeting to achieve effective protection of 10% of the global marine ecoregions by 2020 [21]. Progress have been made, because so far 8.7% of the continental shelf in Kenya, 8.1% in Tanzania, and 4.0% in Mozambique has been designated [22]. The observed pattern of connectivity and the measured genetic diversity can serve to provide useful information for designing MPA networks for protection of biodiversity in the study area. Since signs of overexploitation and historical bottlenecks were observed at each site, special attention should be given to areas which showed low genetic diversity. Considering that the coastal population is growing rapidly, East African countries

should promote sustainable fishing practices and sustainable use of mangrove resources to protect giant mud crabs and other marine fauna from the increasing pressure of exploitation.

Supporting information

S1 Table. Variable sites among the East African *Scylla serrata* COI haplotypes.
(DOCX)

Acknowledgments

The authors are very thankful to the government authorities in the study area for providing the required permits to export samples. The first author also gratefully acknowledges Alex Nehemia and Hajaniaina Ratsimbazafy for their assistance during sampling. Last but not least, the authors are very thankful to the two anonymous reviewers for their constructive remarks.

Author Contributions

Conceptualization: Cyrus Rumisha, Diary Rapanoel, Nemo Mascaux, Marc Kochzius.

Data curation: Cyrus Rumisha, Filip Huyghe, Diary Rapanoel, Nemo Mascaux.

Formal analysis: Cyrus Rumisha, Filip Huyghe, Diary Rapanoel.

Funding acquisition: Cyrus Rumisha, Marc Kochzius.

Investigation: Cyrus Rumisha.

Methodology: Cyrus Rumisha, Filip Huyghe, Nemo Mascaux.

Project administration: Marc Kochzius.

Supervision: Marc Kochzius.

Writing – original draft: Cyrus Rumisha, Diary Rapanoel.

Writing – review & editing: Cyrus Rumisha, Filip Huyghe, Marc Kochzius.

References

1. Richmond MD, editor. A Field Guide to the sea shores of Eastern Africa and the Western Indian Ocean Islands. 2nd ed. Sida/SAREC-UDSM; 2002.
2. Mirera DO. Trends in exploitation, development and management of artisanal mud crab (*Scylla serrata*-Forsskal-1775) fishery and small-scale culture in Kenya: An overview. Ocean Coast Manag. 2011; 54: 844–855. https://doi.org/10.1016/j.ocecoaman.2011.08.001
3. Ewel KC, Rowe S, McNaughton B, Bonine KM. Characteristics of *Scylla* spp. (Decapoda: Portunidae) and their mangrove forest habitat in Ngaremeduu Bay, Republic of Palau. Pacific Sci. 2009; 63: 15–26. https://doi.org/10.2984/1534-6188(2009)63[15:COSSDP]2.0.CO;2
4. Alberts-Hubatsch H, Lee SY, Meynecke J-O, Diele K, Nordhaus I, Wolff M. Life-history, movement, and habitat use of *Scylla serrata* (Decapoda, Portunidae): current knowledge and future challenges. Hydrobiologia. 2016; 763: 5–21. https://doi.org/10.1007/s10750-015-2393-z
5. Meynecke J., Richards R. A full life cycle and spatially explicit individual-based model for the giant mud crab (*Scylla serrata*): a case study from a marine protected area. ICES J Mar Sci. 2014; 71: 484–498. https://doi.org/10.1093/icesjms/fst034
6. Holme M-H, Zeng C, Southgate P. Towards development of formulated diets for mud crab larvae and a better understanding of their nutrional requirements. Aqua Feed Formul Beyond. 2006; 3: 3–6.
7. Rodriguezl SR, Ojedal FP, Inestrosa NC. Settlement of benthic marine invertebrates. 1993; 97: 193–207.
8. Welch JM, Rittschof D, Bullock TM, Forward RB Jr. Effects of chemical cues on settlement behavior of blue crab Callinectes sapidus postlarvae. Mar Ecol Prog Ser. 1997; 154: 143–153.

9. Olsén H. Effects of pollutants on olfactory mediated behaviors in fish and crustaceans. In: Breithaupt T, Thiel M, editors. Chemical Communication in Crustaceans. New York: Springer; 2011. pp. 507–529. https://doi.org/10.1007/978-0-387-77101-4
10. Mirera DO, Ochiewo J, Munyi F, Muriuki T. Heredity or traditional knowledge: Fishing tactics and dynamics of artisanal mangrove crab (*Scylla serrata*) fishery. Ocean Coast Manag. 2013; 84: 119–129. https://doi.org/10.1016/j.ocecoaman.2013.08.002
11. Fondo EN, Kimani EN, Odongo DO. The status of mangrove mud crab fishery in Kenya, East Africa. Int J Fish Aquac. 2010; 2: 79–86.
12. Mwaluma J. Pen culture of the mud crab *Scylla serrata* in Mtwapa mangrove system, Kenya. West Indian Ocean J Mar Sci. 2002; 1: 127–133.
13. Rumisha C, Mdegela RH, Kochzius M, Leermakers M, Elskens M. Trace metals in the giant tiger prawn *Penaeus monodon* and mangrove sediments of the Tanzania coast: is there a risk to marine fauna and public health? Ecotoxicol Environ Saf. 2016; 132: 77–86. https://doi.org/10.1016/j.ecoenv.2016.05.028 PMID: 27281719
14. Rumisha C, Leermakers M, Mdegela RH, Kochzius M, Elskens M. Bioaccumulation and public health implications of trace metals in edible tissues of the crustaceans *Scylla serrata* and *Penaeus monodon* from the Tanzanian coast. Environ Monit Assess. 2017; 189: 529. https://doi.org/10.1007/s10661-017-6248-0 PMID: 28963703
15. FAO. Status and trends in mangrove area extent worldwide. By Wilkie M.L. and Fortuna S. Forest Resources Assessment Working Paper No. 63. Forest Resources Division. Rome, Italy; 2003.
16. Valiela I, Bowen JL, York JK. Mangrove forests: one of the world's threatened major tropical environments. Bioscience. 2001; 51: 807–815. https://doi.org/10.1641/0006-3568(2001)051[0807:MFOOTW]2.0.CO;2
17. Dixon JD, Oli MK, Wooten MC, Eason TH, McCown JW, Cunningham MW. Genetic consequences of habitat fragmentation and loss: the case of the Florida black bear (*Ursus americanus floridanus*). Conserv Genet. 2007; 8: 455–464. https://doi.org/10.1007/s10592-006-9184-z
18. Dixo M, Metzger JP, Morgante JS, Zamudio KR. Habitat fragmentation reduces genetic diversity and connectivity among toad populations in the Brazilian Atlantic Coastal Forest. Biol Conserv. 2009; 142: 1560–1569. https://doi.org/10.1016/j.biocon.2008.11.016
19. Nehemia A, Huyghe F, Kochzius M. Genetic erosion in the snail *Littoraria subvittata* (Reid, 1986) due to mangrove deforestation. J Molluscan Stud. 2017; 83: 1–10. https://doi.org/10.1093/mollus/eyw040
20. Rumisha C, Leermakers M, Elskens M, Mdegela RH, Gwakisa P, Kochzius M. Genetic diversity of the giant tiger prawn *Penaeus monodon* in relation to trace metal pollution at the Tanzanian coast. Mar Pollut Bull. 2017; 114: 759–767. https://doi.org/10.1016/j.marpolbul.2016.10.057 PMID: 27829502
21. MPA news. With global MPA coverage falling short of 10% target, biodiversity summit extends deadline. International News and Analysis on Marine Protected Areas. 2010: 1–8.
22. Wells S, Burgess N, Ngusaru A. Towards the 2012 marine protected area targets in Eastern Africa. Ocean Coast Manag. 2012; 50: 67–83. https://doi.org/10.1016/j.ocecoaman.2006.08.012
23. Allison G., Lubchenco J, Carr M. Marine reserves are necessary but not sufficient for marine conservation. Ecol Appl. 1998; 8: 79–92.
24. Silva IC, Mesquita N, Paula J. Lack of population structure in the fiddler crab *Uca annulipes* along an East African latitudinal gradient: genetic and morphometric evidence. Mar Biol. 2010; 157: 1113–1126. https://doi.org/10.1007/s00227-010-1393-9
25. Silva SE, Silva IC, Madeira C, Sallema R, Paulo OS, Paula J. Genetic and morphological variation in two littorinid gastropods: Evidence for recent population expansions along the East African coast. Biol J Linn Soc. 2013; 108: 494–508. https://doi.org/10.1111/j.1095-8312.2012.02041.x
26. Fratini S, Vannini M. Genetic differentation in the mud crab *Scylla serrata* (Decapoda: Portunidae) within the Indian Ocean. J Exp Mar Bio Ecol. 2002; 272: 103–116.
27. Fratini S, Ragionieri L, Cannicci S. Stock structure and demographic history of the Indo-West Pacific mud crab *Scylla serrata*. Estuar Coast Shelf Sci. 2010; 86: 51–61. https://doi.org/10.1016/j.ecss.2009.10.009
28. Oliveira EC, Österlund K, Mtolera MSP. Marine plants of Tanzania: a field guide to the seaweeds and seagrasses of Tanzania. Sporrong N, Björk M, editors. Stockholm, Sweden: Sida/Department for Research Cooperation, SAREC; 2005.
29. Taylor M, Ravilious C, Green EP. Mangroves of East Africa [Internet]. Cambridge; 2003. Available: http://agris.fao.org/agris-search/search.do?recordID=XF2015021752
30. Rumisha C, Shukuru H, Lyimo J, Maganira J, Nehemia A. Benthic macroinvertebrate assemblages in mangroves and open intertidal areas on the Dar es Salaam coast, Tanzania. African J Aquat Sci. 2015; 40: 143–151. https://doi.org/10.2989/16085914.2015.1051504

31. Schott FA, McCreary JP. The monsoon circulation of the Indian Ocean. Prog Oceanogr. 2001; 51: 1–123. https://doi.org/10.1016/S0079-6611(01)00083-0

32. Schouten MW, De Ruijter WPM, Van Leeuwen PJ, Ridderinkhof H. Eddies and variability in the Mozambique Channel. Deep Res II. 2003; 50: 1987–2003. https://doi.org/10.1016/S0967-0645(03)00042-0

33. Gopurenko D, Hughes JM, Keenan CP. Mitochondrial DNA evidence for rapid colonisation of the Indo-West Pacific by the mudcrab *Scylla serrata*. Mar Biol. 1999; 134: 227–233. https://doi.org/10.1007/s002270050541

34. Fuseya R, Sakamoto T, Dan S, Tamaki M, Hayashibara T, Katoh M. Development and characterization of microsatellite markers from mud crab *Scylla serrata* for population genetics. Aquaculture. 2007; 272: 38–57. https://doi.org/10.1016/j.aquaculture.2007.07.063

35. Yao HF, Sun DQ, Wang RX, Shi G. Rapid isolation and characterization of polymorphic microsatellite loci in the mud crab, *Scylla paramamosain* (Portunidae). Genet Mol Res. 2012; 11: 1503–1506. https://doi.org/10.4238/2012.May.21.7 PMID: 22653600

36. Ma H, Ma C, Ma L. Identification of type I microsatellite markers associated with genes and ESTs in *Scylla paramamosain*. Biochem Syst Ecol. 2011; 39: 371–376. https://doi.org/10.1016/j.bse.2011.05.007

37. Holleley CE, Geerts PG. Multiplex Manager 1.0: A cross-platform computer program that plans and optimizes multiplex PCR. Biotechniques. 2009; 46: 511–517. https://doi.org/10.2144/000113156 PMID: 19594450

38. Glaubitz JC. CONVERT: a user-friendly program to reformat diploid genotypic data for commonly used population genetic software packages. Mol Ecol Notes. 2004; 4: 309–310. https://doi.org/10.1111/j.1471-8286.2004.00597.x

39. Roehrdanz RL. An improved primer for PCR amplification of mitochondrial DNA in a variety of insect species. Insect Mol Biol. 1993; 2: 89–91. https://doi.org/10.1111/j.1365-2583.1993.tb00129.x PMID: 9087547

40. Tamura K, Stecher G, Peterson D, Filipski A, Kumar S. MEGA6: molecular evolutionary genetics analysis version 6.0. Mol Biol Evol. 2013; 30: 2725–2729. https://doi.org/10.1093/molbev/mst197 PMID: 24132122

41. Alcazar DSR, Kochzius M. Genetic population structure of the blue sea star *Linckia laevigata* in the Visayas (Philippines). J Mar Biol Assoc United Kingdom. 2015; 96: 707–713. https://doi.org/10.1017/S0025315415000971

42. Peakall R, Smouse PE. GenAlEx 6.5: genetic analysis in Excel. Population genetic software for teaching and research-an update. Bioinformatics. 2012; 28: 2537–2539. https://doi.org/10.1093/bioinformatics/bts460 PMID: 22820204

43. Goudet J. FSTAT (version 1.2): a computer program to calculate F-Statistics. J Hered. 1995; 86: 485–486.

44. Van Oosterhout C, Hutchinson WF, Wills DPM, Shipley P. MICRO-CHECKER: software for identifying and correcting genotyping errors in microsatellite data. Mol Ecol Notes. 2004; 4: 535–538. https://doi.org/10.1111/j.1471-8286.2004.00684.x

45. Librado P, Rozas J. DnaSP v5: a software for comprehensive analysis of DNA polymorphism data. Bioinformatics. 2009; 25: 1451–1452. https://doi.org/10.1093/bioinformatics/btp187 PMID: 19346325

46. Excoffier L, Lischer HEL. Arlequin suite ver 3.5: a new series of programs to perform population genetics analyses under Linux and Windows. Mol Ecol Resour. 2010; 10: 564–567. https://doi.org/10.1111/j.1755-0998.2010.02847.x PMID: 21565059

47. Wang J. Does GST underestimate genetic differentiation from marker data? Mol Ecol. 2015; 24: 3546–3558. https://doi.org/10.1111/mec.13204 PMID: 25891752

48. Holm S. A simple sequentially rejective multiple test procedure. Scand J Stat. 1979; 6: 65–70. https://doi.org/10.2307/4615733

49. Pritchard JK, Stephens M, Donnelly PJ. Inference of population structure using multilocus genotype data. Genetics. 2000; 155: 945–959. https://doi.org/10.1002/spe.4380060305 PMID: 10835412

50. Evanno G, Regnaut S, Goudet J. Detecting the number of clusters of individuals using the software STRUCTURE: a simulation study. Mol Ecol. 2005; 14: 2611–2620. https://doi.org/10.1111/j.1365-294X.2005.02553.x PMID: 15969739

51. Villesen P. FaBox: an online toolbox for FASTA sequences. Mol Ecol Notes. 2007; 7: 965–968. https://doi.org/10.1111/j.1471-8286.2007.01821.x

52. Leigh JW, Bryant D. Popart: full-feature software for haplotype network construction. Methods Ecol Evol. 2015; 6: 1110–1116. https://doi.org/10.1111/2041-210X.12410

53. Beerli P, Palczewski M. Unified framework to evaluate panmixia and migration direction among multiple sampling locations. Genetics. 2010; 185: 313–326. https://doi.org/10.1534/genetics.109.112532 PMID: 20176979

54. Fu XY. Statistical tests of neutrality of mutations against population growth, hitchhiking and background selection. Genetics. 2007; 147: 915–925.

55. Tajima F. Statistical method for testing the neutral mutation hypothesis by DNA polymorphism. Genetics. 1989; 123: 585–595. PMC1203831 PMID: 2513255

56. Harpending HC. Signature of ancient population growth in a low-resolution mitochondrial DNA mismatch distribution. Hum Biol. 1994; 66: 591–600. PMID: 8088750

57. Alves MJ, Coelho H, Collares-Pereira MJ, Coelho MM. Mitochondrial DNA variation in the highly endangered cyprinid fish *Anaecypris hispanica*: importance for conservation. Heredity (Edinb). 2001; 87: 463–473. https://doi.org/10.1046/j.1365-2540.2001.00929.x

58. Fratini S, Ragionieri L, Cannicci S. Demographic history and reproductive output correlates with intraspecific genetic variation in seven species of Indo-Pacific mangrove crabs. PLoS One. 2016; 11: e0158582. https://doi.org/10.1371/journal.pone.0158582 PMID: 27379532

59. Frankham R. Genetics and extinction. Biol Conserv. 2005; 126: 131–140. https://doi.org/10.1016/j.biocon.2005.05.002

60. Ferreri M, Qu W, Han B. Phylogenetic networks: a tool to display character conflict and demographic history. African J Biotechnol. 2011; 10: 12799–12803. https://doi.org/10.5897/AJB11.010

61. Hewitt G. The genetic legacy of the Quaternary ice ages. Nature. 2000; 405: 907–913. https://doi.org/10.1038/35016000 PMID: 10879524

62. Karl SA, Toonen RJ, Grant WS, Bowen BW. Common misconceptions in molecular ecology: echoes of the modern synthesis. Mol Ecol. 2012; 21: 4171–4189. https://doi.org/10.1111/j.1365-294X.2012.05576.x PMID: 22574714

63. Weng ZH, Xie YJ, Xiao ZQ, Wang ZY, Gui JF. Microsatellite and mitochondrial DNA analysis of the genetic structure of Chinese horseshoe crab (*Tachypleus tridentatus*) in southeast China coast. African J Biotechnol. 2013; 12: 2088–2099. https://doi.org/10.5897/AJB12.1912

64. Martien KK, Chivers SJ, Baird RW, Archer FI, Gorgone AM, Hancock-Hanser BL, et al. Nuclear and Mitochondrial Patterns of Population Structure in North Pacific False Killer Whales (*Pseudorca crassidens*). J Hered. 2014; 105: 611–626. https://doi.org/10.1093/jhered/esu029 PMID: 24831238

65. Humphries EM, Winker K. Discord reigns among nuclear, mitochondrial and phenotypic estimates of divergence in nine lineages of trans-Beringian birds. Mol Ecol. 2011; 20: 573–583. https://doi.org/10.1111/j.1365-294X.2010.04965.x PMID: 21199027

66. Avise JC. Molecular markers, natural history, and evolution. 2nd ed. Sunderland, Massachusetts: Sinauer Associates, Inc.; 2004.

67. Larsson LC, Charlier J, Laikre L, Ryman N. Statistical power for detecting genetic divergence—organelle versus nuclear markers. Conserv Genet. 2009; 10: 1255–1264. https://doi.org/10.1007/s10592-008-9693-z

68. Bonine KM, Bjorkstedt EP, Ewel KC, Palik M. Population characteristics of the mangrove crab *Scylla serrata* in Kosrae, Federated States of Micronesia: effects of harvest and implications for management. Pacific Sci. 2007; 62: 1–19. https://doi.org/10.2984/1534-6188(2008)62[1:pcotmc]2.0.co;2